

# A FORWARD MODEL OF LIMB INFRARED EMISSION SPECTRA IN A TWO-DIMENSIONAL ATMOSPHERE

Coralie De Clercq<sup>(1)</sup> and Jean-Christopher Lambert<sup>(1)</sup>

(1) Belgian Institute for Space Aeronomy (IASB-BIRA), Avenue Circulaire 3, B-1180 Brussels (Uccle), Belgium

## ABSTRACT

Most frequently, one-dimensional profiles of atmospheric constituents are retrieved from satellite radiance measurements assuming a spherical atmosphere made of homogeneous, concentric layers. Averaging kernels associated with the retrieval enable one-dimensional characterisation of the retrieved information as a function of altitude or pressure. Nevertheless, two-dimensional characterisation of the information retrievable from satellite measurements is highly desirable for an increasing number of scientific and operational applications. We describe here a simple radiative transfer model capable of calculating limb radiance emission spectra in a two-dimensional atmosphere. Radiative transfer basics resemble those adopted in the operational processing of Envisat Michelson Interferometer for Passive Atmospheric Sounding (MIPAS) data. However, to keep it as fast and flexible as possible, the model assumes several simplifications having no or weak influence on geometrical aspects of the ray tracing. The model is applied to MIPAS particulars (limb scanning strategy, global fit retrieval approach, specific spectral microwindows) in order to investigate the two-dimensional distribution of the sounded information.

## 1 INTRODUCTION

Measurement of the vertical distribution and variability of key trace species in the global stratosphere is required in the current context of global changes of atmospheric composition and climate. Among the various observation techniques yielding access to global, height-resolved information on atmospheric temperature and trace species abundances, limb sounding of atmospheric emission spectra from an orbiting platform combines the advantages of a good vertical resolution and of a good signal-to-noise ratio resulting from long path lengths. However, three effects counteract those advantages by producing a poor horizontal or, in Earth-centred coordinates, angular resolution. First, limb radiance spectra are the result of emissions and absorptions competing along the long optical paths. Moreover, during a full limb-scanning sequence from high to low altitudes, the same atmospheric layer is intersected several times by different optical paths. Furthermore, successive tangent points follow the satellite in its orbital plane. Consequently, the information available at the end of the full sequence is distributed not only vertically but also angularly (see Fig. 1).

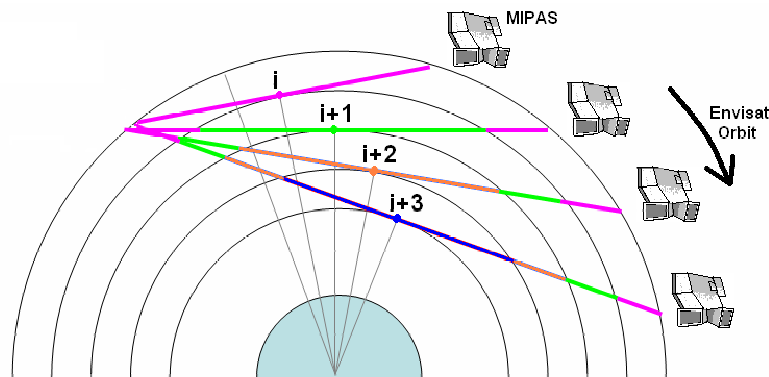


**Fig. 1.** Geometrical illustration of the information sounded by MIPAS during four successive limb measurements (tangent altitudes  $i$  down to  $i+3$ ) in backward viewing mode. Successive tangent points follow the orbital progression of Envisat. The atmospheric layer between tangent points  $i$  and  $i+1$  is intersected by all individual scans from tangent altitude  $i+1$  down to the lowest tangent altitude.

We have developed a simple forward model capable of calculating limb radiance emission spectra in a two-dimensional, inhomogeneous atmosphere, and taking into account the orbital motion of the instrument. Two mid-infrared limb sounders are currently in operation: Michelson Interferometer for Passive Atmospheric Sounding (MIPAS) [1] aboard ESA's environmental satellite Envisat since 2002 and Tropospheric Emission Spectrometer (TES) [2] aboard NASA's atmospheric research satellite Aura since 2004. In this paper, we have adapted the forward model to MIPAS/Envisat particulars and investigated the two-dimensional distribution of the information available after a full limb-scanning sequence of this instrument. The model is described in Section 3, while the information actually sounded is characterised in Section 4. This study focuses on the detection of carbon dioxide spectra ( $\text{CO}_2$ ), from which MIPAS temperature profile data are retrieved. As MIPAS data processors use temperature retrievals later for the retrieval of other species, conclusions drawn in Section 5 should impact the retrieval of other species as well.

## 2 MIPAS OPERATION AND DATA PROCESSING

The MIPAS instrument [1] is a cooled, high resolution Fourier Transform Spectrometer designed for the detection of limb emission spectra in the middle and upper atmosphere. Four spectral channels cover the middle infrared spectral range from  $650 \text{ cm}^{-1}$  to  $2400 \text{ cm}^{-1}$  at about  $0.025 \text{ cm}^{-1}$  resolution, allowing the detection of a bouquet of atmospheric species including ozone ( $\text{O}_3$ ), water vapour ( $\text{H}_2\text{O}$ ), nitrogen oxides ( $\text{NO}$ ,  $\text{NO}_2$ ,  $\text{N}_2\text{O}_5$ ), source gases ( $\text{CH}_4$ ,  $\text{N}_2\text{O}$ ,  $\text{CO}$ ), nitrogen and chlorine reservoirs ( $\text{ClONO}_2$ ,  $\text{HNO}_3$ ,  $\text{HCl}$ ...), and CFCs. A complete limb-scanning sequence spans vertically the atmosphere from 68 km down to 6 km in tangent altitude, with a vertical spacing between successive measurements of 3 km in the troposphere and stratosphere and a coarser spacing above. The instrument operates aboard Envisat, a polar platform (orbit inclination of  $98.6^\circ$ ) flying at a mean altitude of 800 km with sun-synchronous precession. Every 100 min, Envisat crosses the descending node at the mean solar time of 10:00 am. For about 80% of its measuring time, MIPAS operates in the so-called nominal observation mode, that is, backward viewing along track. Additionally, the so-called special modes are designed for the study of specific geographic regions (e.g. polar regions in winter time) or special events (such as volcanic eruptions).

Vertical distributions of pressure, temperature and mixing ratio of six high-priority species ( $\text{O}_3$ ,  $\text{H}_2\text{O}$ ,  $\text{HNO}_3$ ,  $\text{CH}_4$ ,  $\text{N}_2\text{O}$  and  $\text{NO}_2$ ) are retrieved from MIPAS spectra by two operational data processors developed under ESA's responsibility, one in near real time (NRT) and one off-line (OFL). Current algorithms do not take into account potential two-dimensional effects. ESA processors generate profile data for the nominal observation mode, while for the special modes only calibrated spectra are provided to the end users. Profile retrieval algorithms are based on multiple line fitting in a set of optimised spectral microwindows and on the global fit approach [3-5]. With this particular approach, the one-dimensional vertical profile of a given species is retrieved from the simultaneous analysis of all spectral measurements acquired during an entire limb-scanning sequence. The global fit provides a comprehensive exploitation of the available information and a rigorous determination of the correlations between atmospheric parameters at the different altitudes. It also permits the full exploitation of hydrostatic equilibrium condition and is better compatible with the modelling of the finite field of view of the instrument.

## 3 TWO-DIMENSIONAL FORWARD MODEL

In order to determine the distribution of information sounded within a complete limb-scanning sequence, we have developed a MIPAS forward model capable of calculating limb radiance spectra in a two-dimensional atmosphere. The model takes into account the particular limb-scanning strategy of the instrument and its motion along the Envisat orbit.

### 3.1 Radiative transfer

Radiative transfer basics resemble those adopted for operational MIPAS data processing [4-6]. Infrared radiance spectra  $L$  in  $\text{W}/(\text{cm}^2 \cdot \text{sr} \cdot \text{cm}^{-1})$  emitted and absorbed at wave number  $\nu$  ( $\text{cm}^{-1}$ ) by a given molecule along the limb optical path  $s$ , are calculated for an observer  $Obs.$  using Eq. 1,

$$L_{\nu, Obs.}(z_{tg}) = \int_{Obs.}^{-\infty} k_{\nu}(s_{tg}) B_{\nu}(T(s_{tg})) \cdot \exp\left(-\int_{Obs.}^{s_{tg}} k_{\nu}(x_{tg}) dx_{tg}\right) ds_{tg} \quad (1)$$

where  $S_{ig}$  and  $X_{ig}$  are line-of-sight coordinates along the optical path with tangent point altitude  $Z_{ig}$ ,  $B_\nu$  is the spectral radiance emitted by Planck's black body source at temperature  $T$ , and  $k_\nu$  ( $\text{m}^{-1}$ ) is the absorption coefficient of the species derived from the high-resolution molecular absorption database HITRAN2004 [7-8]. To keep the model as fast and flexible as possible, several details having no or weak influence on geometrical aspects of the ray tracing and total radiance have been omitted. Scattering by air and by particles in the stratosphere and upper troposphere usually can be neglected in the middle infrared in the absence of optically thick clouds and aerosols with large albedo [9]. Local thermodynamic equilibrium (LTE) is assumed at all altitudes, although non-LTE conditions occur already in the upper stratosphere for a few molecules like NO, NO<sub>2</sub>, CO and H<sub>2</sub>O. Full line-by-line computation is performed for every MIPAS micro-window. Ray tracing is performed for every tangent altitude. Optical bending by atmospheric refraction is calculated apart as a function of pressure and temperature. Instrumental effects linked e.g. to the finite instrument field of view or the instrument line shape are not taken into account as they influence mostly the spectral fitting and the accuracy of the retrievals [4].

### 3.2 Description of the atmosphere

The atmosphere is modelled as a compilation of 120 concentric isobars, extending from the ground up to the top of atmosphere (TOA) fixed at 120 km. With respect to conventional forward models, as the one adopted for the MIPAS operational processors, a major difference consists in the fact that ray tracing is performed in a fully two-dimensional atmosphere, in Earth-centred radial and angular coordinates. The angular plane is determined by the Envisat orbit. For simulations in an atmosphere made of homogeneous layers, vertical distributions of pressure, temperature and atmospheric emitters are selected from well-documented sources such as the AFGL atmospheric profile database [10] and the COSPAR International Reference Atmosphere CIRA [11-12]. For simulations in an inhomogeneous and changing atmosphere, three-dimensional atmospheric fields generated by ECMWF and by the BASCOE assimilation system [13-14] can be interfaced with the radiative transfer module to incorporate angular inhomogeneities, as well as short-term variability on the timescale of hours. Higher-frequency variability – resulting e.g. from non-stationary effects during one interferometer sweep – is not taken into account.

### 3.3 Limb-scanning sequence and orbital progression

A complete limb-scanning sequence spans vertically the atmosphere from 68 km down to 6 km in tangent altitude, with a vertical spacing between successive measurements of 3 km in the troposphere and stratosphere and a coarser spacing above. Downward scanning is associated with a retrograde motion of tangent points with respect to the satellite, of about 1.1 degree between the upper (at 68 km) and lowest (at 6 km) tangent points of the sequence. The satellite itself orbits in the opposite direction at a speed of about 7.45 km/s. At the end of a complete sequence (72 s), the satellite has progressed of 4.28 degree along its orbit. The net effect is an angular spacing of about 3.18 degree in the orbit plane between the upper and lowest tangent points of the sequence.

## 4 INFORMATION SOUNDED DURING A MIPAS SEQUENCE

### 4.1 Sequence of individual limb radiance measurements

Fig. 2 shows limb radiances calculated at a selection of tangent altitudes from 68 km to 6 km, for two CO<sub>2</sub> spectral microwindows. The first one, MW2 (686.4-689.4  $\text{cm}^{-1}$ ), is used by ESA's off-line processor to retrieve temperature profile data in the 30-68 km altitude range, while the second one, MW 8 (791.375-792-875  $\text{cm}^{-1}$ ), is used for the 6-33 km range.

### 4.2 Contribution functions along a single optical path

For the two same microwindows, and as a function of the tangent altitude, Fig. 3 (left part) displays the contribution of each optical path element to the total CO<sub>2</sub> radiance observed by MIPAS. Each contribution is the net balance between the local emission and the absorption occurring between the emitter and the satellite. At this stage, geometrical effects are not taken into account yet.

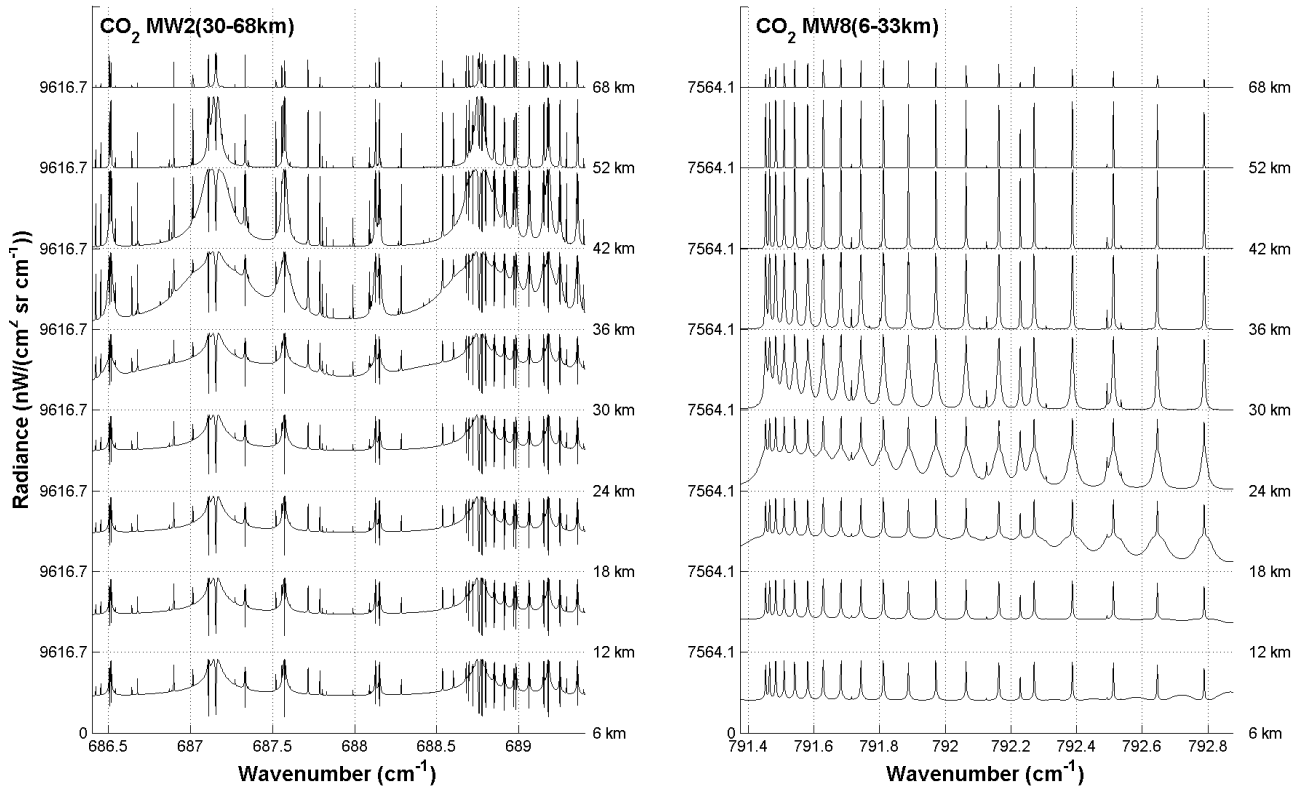


**Fig. 2.** Synthetic CO<sub>2</sub> radiances measured during a MIPAS limb-scanning sequence (tangent point sampling the limb at altitudes from 68 km down to 6 km) in microwindows 2 (left, used for retrievals at 30-68 km) and 8 (right, used for retrievals at 6-33 km).

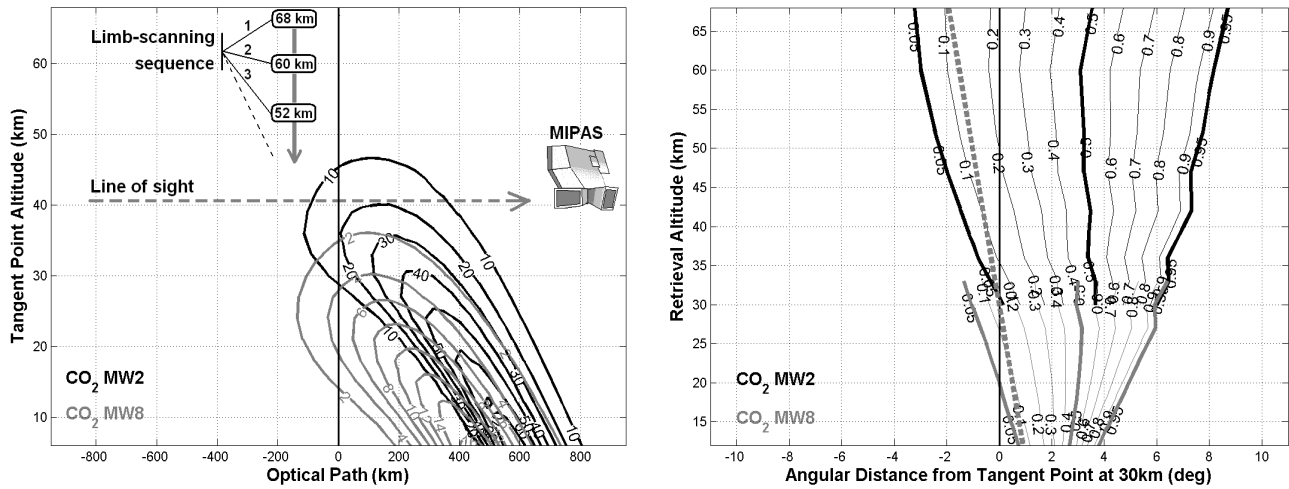


**Fig. 3.** Left: Line-of-sight contribution to the CO<sub>2</sub> limb radiance (in W/cm<sup>2</sup>.sr.km) calculated in MW2 and MW8, and displayed as a function of tangent altitude and optical path distance from tangent point. Right: for the same microwindows MW2 and MW8, angular distribution of the normalised, cumulative CO<sub>2</sub> limb radiance calculated now for a full limb sequence, and displayed as a function of retrieval altitude and angular coordinate. Thick, continuous contours indicate the 5%, 50% and 95% contribution levels. The angular origin is the vertical crossing the tangent point chosen arbitrarily at 30 km. The thick, dashed grey line indicates the contribution of the orbital motion of Envisat.

### 4.3 Contribution functions for a full sequence

We take now into account radiances measured during an entire limb-scanning sequence. We include additional geometrical effects through a change of coordinates, from MIPAS measurement space to Earth-centred space: (optical path/tangent altitude) coordinates become (angular distance/retrieval altitude) coordinates. Satellite motion effects can be included at this stage. Fig. 3 (right part) shows the angular and vertical distribution of contributions to the entire limb-scanning sequence of CO<sub>2</sub> radiances for MW2 and MW8. Contribution functions are expressed here as the normalised, cumulative radiance corresponding to each retrieval altitude.

## 5 RESULTS AND CONCLUSION

A common assumption for limb-sounded data is that most of the measured information concentrates around the tangent point. This assumption is not accurate. According to Fig. 3, air masses generating CO<sub>2</sub> radiances actually measured by MIPAS are located between the tangent point and the satellite. The reason is that radiation emitted at this particular location experiences less absorption along its path to the satellite, than radiation emitted before the tangent point. The median contribution to the observed radiances (50% of cumulative radiance) is located at about 3 degree away from the vertical crossing the tangent point at 30 km. Fig. 3 also shows that the sounded information spreads around the median location. For geometrical reasons (see Fig. 1), this angular spread increases logically with altitude, higher altitudes being intersected by many more tangent rays than lower altitudes. As a result, the 90% spread of the cumulative radiance increases from 3.5 degree at the tropopause to 10 degree above the stratopause. The angular distance and spread of the sounded information have consequences for a variety of applications where effective geolocation of the retrieved data matters.

## 6 ACKNOWLEDGEMENTS

The authors address their thanks to the BASCOE team at IASB-BIRA for providing modelling data and the MIPAS team at IMK/FZK for fruitful discussions. This work was funded by the Belgian Federal Science Policy Office and the European Space Agency via the PRODEX project C15151 P7/P8 (CINAMON).

## 7 REFERENCES

1. Fischer, H., and H. Oelhaf, Remote sensing of vertical profiles of atmospheric trace constituents with MIPAS limb-emission spectrometers, *Appl. Opt.*, Vol. 35, No. 16, 2787-2796, 1996.
2. Beer, R., T. A. Glavich, and D. M. Rider, Tropospheric emission spectrometer for the Earth Observing System's Aura satellite, *Appl. Opt.*, Vol. 40, 2356-2367, 2001.
3. Carlotti, M., Global-fit approach to the analysis of limb-scanning atmospheric measurements, *Appl. Opt.*, Vol. 27, 3250, 1988.
4. Carlotti, M., M. Höpfner, P. Raspollini, and M. Ridolfi, Development of an optimised algorithm for routine p, T and VMR retrieval from MIPAS limb emission spectra: High level algorithm definition and physical and mathematical optimisations, ESA/IROE Technical Note TN-IROE-RSA9601, Issue 2 Rev. A, 79 pp., 20/10/1998.
5. ESA, The Michelson Interferometer for Passive Atmospheric Sounding: An instrument for Atmospheric Chemistry and Climate Research, European Space Agency Scientific Publication, SP-1229, 124 pp., March 2000.
6. Ridolfi, M., B. Carli, T. v. Clarmann, B. M. Dinelli, A. Dudhia, et al., Optimized forward model and retrieval scheme for MIPAS near-real-time data processing, *Appl. Opt.*, Vol. 39, 1323-1340, 2000.
7. Rothman, L. S., A. Barbe, D. Chris Benner, L. R. Brown, C. Camy-Peyret, et al., The HITRAN molecular spectroscopic database: edition of 2000 including updates through 2001, *J. Quant. Spectros. Rad. Transf.*, Vol. 82, 5-44, 2003.
8. Rothman, L. S., D. Jacquemart, A. Barbe, D. Chris Benner, M. Birk, et al., The HITRAN 2004 molecular spectroscopic database, *J. Quant. Spectros. Rad. Transf.*, Vol. 96, 139-204, 2005.
9. Höpfner, M., and C. Emde, Comparison of single and multiple scattering approaches for the simulation of limb-emission observations in the mid-IR, *J. Quant. Spectros. Rad. Transf.*, Vol. 91, 275-285, 2005.

10. Anderson, G. P., S.A. Clough, F. X. Kneizys, J. H. Chetwynd, and E. P. Shettle, AFGL Atmospheric Constituents Profiles (0-120 km), Environmental Research Papers, No. 954, AFGL-TR-86-0110, AFGL (OPI), Hanscom AFB, MA 01736, 1986.
11. [Fleming, E.L., S. Chandra, J.J. Barnett, and M. Corney, COSPAR International Reference Atmosphere, Chapter 2: Zonal mean temperature, pressure, zonal wind and geopotential height as functions of latitude, \*Adv. Space Res.\*, 10\(12\), pp. 11-59, 1990.](#)
12. [Keating, G.M., J.S. Chiou and N.C. Hsu, Improved ozone reference models for the COSPAR International Reference Atmosphere, \*Adv. Space Res.\*, Vol. 18, No. 9/10, 11-58, 1996.](#)
13. [Errera, Q., and D. Fonteyn, Four-dimensional variational chemical assimilation of CRISTA stratospheric measurements, \*J. Geophys. Res.\*, Vol. 106, 12,253-12,265, 2001.](#)
14. [Fonteyn, D., S. Bonjean, S. Chabrillat, F. Daerden, and Q. Errera, 4D-VAR chemical data assimilation of ENVISAT chemical products \(BASCOE\): Validation support issues, in \*Proc. Envisat Validation Workshop\*, ESA Scientific Publication SP-531, 2003.](#)